
Go Beyond Your Means: Unlearning with Per-Sample Gradient Orthogonalization

Aviv Shamsian^{*1} Eitan Shaar^{*2} Aviv Navon² Gal Chechik^{1,3} Ethan Fetaya¹

Abstract

Machine unlearning aims to remove the influence of problematic training data after a model has been trained. The primary challenge in machine unlearning is ensuring that the process effectively removes specified data without compromising the model’s overall performance on the remaining dataset. Many existing machine unlearning methods address this challenge by carefully balancing gradient ascent on the ‘unlearn’ data with the gradient descent on a ‘retain’ set representing the training data. Here, we propose OrthoGrad, a novel approach that mitigates interference between the unlearn set and the retain set rather than competing ascent and descent processes. Our method projects the gradient of the unlearn set onto the subspace orthogonal to all gradients in the retain batch, effectively avoiding any gradient interference. We demonstrate the effectiveness of OrthoGrad on multiple machine unlearning benchmarks, including automatic speech recognition, outperforming competing methods.

1. Introduction

Foundational models, i.e., machine learning models trained on enormous datasets, have led to breakthroughs in various tasks (Brown et al., 2020; Radford et al., 2021; 2023). Due to the scale of these datasets, the data-gathering process is automated, usually by scrapping diverse web content, and not curated by people. As a result, problematic data often leaks into training datasets, and may contaminate model training. Contaminated data may be due to copyright content or illegal one. For example, Github Copilot (Dakhel et al., 2023; Siroš et al., 2024) faced criticism for generating code snippets directly from open-source repositories without attribution, leading to legal disputes about copyright violations. As another example, LAION-5B (Schuhmann

et al., 2022), a 5.85 billion image-text pairs dataset, had to be temporarily removed when it was discovered it contained CSAM images (Thiel, 2023). Another concern is privacy: training data may contain private information, which can be extracted by users with access to the model, potentially leaking sensitive data (Carlini et al., 2021). Finally, considering the point of view of an individual application, users may ask to ‘opt out’ and to not be recognized by the system. For example, a user might want a speech recognition system to not transcribe his audio recordings.

A naive approach to address undesirable data, once identified, is to remove them from the training dataset and retrain the model. Clearly, this may be too expensive in time, power and money (many LLMs may cost 100M\$ or more to train). Additionally, a contaminated model may be a finetuned version of a base model shared online, in which case its original training datasets are often kept private. As a result, developers aiming to mitigate the influence of unwanted data for their specific applications may lack access to the original dataset required for retraining. This highlights the need for efficient post-training solutions that do not rely on large retrain data.

These challenges led to a growing recent interest in *machine unlearning* (Liu et al., 2024; Nguyen et al., 2022). In this setup, we wish to remove the effects of a given part of the training data on a given pretrained model while preserving its generalization performance. In this framework, we are given an *unlearn set* we wish to forget, and a *retain set* which represents the training data. Many existing methods (Kurmanji et al., 2024; Lin et al., 2024) tackle the unlearning problem by combining gradient ascent on the unlearn set to degrade the model performance on these data points with gradient descent on the retain set to preserve its performance on unseen data. Although these approaches have shown promising results, many depend on having a large retain set, leading to poor performance when only a limited amount of data is available. In real-world scenarios, access to extensive training data is often restricted, such as in proprietary datasets used by companies or confidential medical records. In such cases, unlearning methods must be effective even with a small dataset.

In this work, we tackle the challenge of machine unlearning

^{*}Equal contribution ¹Bar Ilan University ²Independent Researcher ³NVIDIA Research. Correspondence to: Aviv Shamsian <aviv.shamsian@live.biu.ac.il>.

in scenarios where access to the retain set is limited. To address this issue, we propose a novel algorithm named *OrthoGrad*, which enables effective unlearning while minimizing the impact on the model’s generalization performance. Rather than relying heavily on the retain set to offset the negative effects of the unlearning process, our method focuses on directly mitigating interference effects at their source.

To motivate our approach, the ideal solution to the unlearning problem should alter the model output for the unlearn set without changing its performance on the retain set. Intuitively, this would be equivalent to an optimization process on the manifold of parameters that yield unaltered performance on all points in the retain set. We use this intuition to design an algorithm that approximates the optimization trajectory on that manifold in a computationally efficient manner. In practice, this is equivalent to projecting the unlearn gradient onto the subspace orthogonal to the gradients of each individual sample in the retain batch. This ensures that the optimization dynamics of the unlearn set are decoupled from those of the retain set, effectively reducing gradient interference (Liu et al., 2021a). Unlike existing methods, which typically operate on the average gradient of the retain batch, our approach takes a *per-sample gradient* perspective, providing a more robust solution to unlearning (Figure 1).

In our experiments, we focus on the challenging regime of low-data scenarios, where access to the retain dataset is significantly limited. These settings highlight the practical constraints often encountered in real-world applications of machine unlearning. We thoroughly evaluate the effectiveness of our approach, OrthoGrad, across several challenging tasks, including image classification and automatic speech recognition. Furthermore, we explore its performance under different unlearning setups, such as random data removal and class-specific forgetting, to demonstrate its versatility. Our results consistently show that OrthoGrad achieves reliable unlearning while maintaining the overall model performance better than other leading unlearning methods.

2. Related Work

The development of efficient machine unlearning methods (Cao & Yang, 2015; Fan et al., 2025; Ginart et al., 2019; Goel et al., 2022; Zhang et al., 2024; Romero et al., 2007; Mehta et al., 2022; Huang et al., 2025) has gained significant attention, addressing a range of applications across domains such as regression tasks (Thudi et al., 2022), federated learning (Liu et al., 2021b; 2022; Wang et al., 2022), graph neural network (Chen et al., 2022; Cheng et al., 2023). Retraining the model from scratch, widely regarded as the gold standard for unlearning (Fan et al., 2023), guarantees the complete removal of data influence. However, this approach is often impractical in production environments due

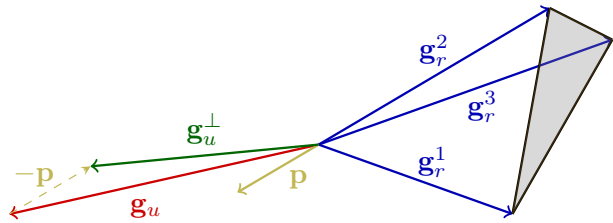


Figure 1. Illustration of the gradient orthogonalization process. The retain gradients \mathbf{g}_r^1 , \mathbf{g}_r^2 , and \mathbf{g}_r^3 (in blue) span a subspace (gray triangle). The projection vector \mathbf{p} (in yellow) is obtained by applying QR decomposition on the retain gradients. The unlearn gradient \mathbf{g}_u is projected using \mathbf{p} to form unlearning gradient which is orthogonal to the retain subspace, \mathbf{g}_u^\perp .

to the extensive computational resources and time required, especially for large-scale datasets. Alternatively, fine-tuning a model for a new task may induce catastrophic forgetting (Lopez-Paz & Ranzato, 2017), but this mechanism fails to ensure the precise removal of specific data influences.

Most machine learning methods leverage techniques like influence functions (Guo et al., 2019; Neel et al., 2021; Wu et al., 2022; Wu & Harandi, 2025; Sekhari et al., 2021), probabilistic approaches (Golatkar et al., 2020b; 2021). However, these methods often face inherent limitations that reduce their practical effectiveness, particularly in defending against membership inference attacks (Dwork et al., 2006; Graves et al., 2021). As a result, the focus has shifted toward developing more effective and efficient unlearning strategies (Golatkar et al., 2020a; Becker & Liebig, 2022; Jia et al., 2023; Chen et al., 2023).

While these approaches represent significant advancements in machine unlearning, many rely on assumptions or techniques that limit their practicality in real-world scenarios. For instance, DUCK (Cotogni et al., 2023), a cluster-based unlearning method, lacks a clear strategy for adapting to auto-regressive models, making it unsuitable for tasks with sequential dependencies. Similarly, SCRUB (Kurmanji et al., 2024), a teacher-student unlearning framework, effectively removes specific data influences but struggles to generalize to diverse setups, such as forgetting a random set of samples. Furthermore, GDR-GMA (Lin et al., 2024)’s reliance on orthogonal projections of averaged gradients fails to account for individual sample variability, leaving residual data influence and reducing unlearning effectiveness.

Although most machine learning methods have been designed for classification tasks, (Fan et al., 2023) emphasize their limitations in addressing unlearning for image generation, a crucial area for safeguarding copyrights and preventing inappropriate outputs.

Table 1. Ablation Study. Evaluation of OrthoGrad variants on ASR unlearning. Values are averaged over 5 different speakers.

	\mathcal{W}_{retain}	$\mathcal{W}_{unlearn}$	$\mathcal{W}_{speaker}$	\mathcal{W}_{test}
OrthoGrad Mean	27.23 ± 11.36	96.67 ± 6.02	64.25 ± 35.48	29.42 ± 14.07
OrthoGrad Per-sample	18.71 ± 4.04	100.00 ± 0.00	96.40 ± 7.04	26.87 ± 0.60
OrthoGrad Mean + Lora	23.77 ± 9.62	92.12 ± 7.34	63.27 ± 35.43	41.21 ± 25.67
OrthoGrad Per-sample + Lora	12.73 ± 1.43	98.30 ± 2.50	81.16 ± 23.97	16.36 ± 0.32
OrthoGrad	12.11 ± 0.65	96.24 ± 8.06	98.53 ± 3.28	13.98 ± 0.58

2.1. Conflicting Gradients in Multi-Task Learning

Multi-task learning (MTL) aims to improve model generalization by optimizing multiple related tasks (Crawshaw, 2020; Zhang & Yang, 2021). However, different tasks often compete for model capacity and produce gradients pointing in opposite directions during training (Yu et al., 2020). This phenomenon, known as gradient interference of conflict, occurs when a gradient that benefits one task degrades the performance of others. Addressing this issue by mitigating these conflicts has become crucial for training MTL systems, with early works focusing on analyzing conflict patterns and their relationships (Sener & Koltun, 2018; Chen et al., 2018). Various optimization-based approaches have been proposed including gradient projection and dropping to reduce task interference (Chen et al., 2020; Wang et al., 2021; Liu et al., 2021a). Recently, geometric and game-theory perspectives have led to methods seeking optimal Pareto solutions in the MTL optimization landscape (Navon et al., 2022; Javaloy & Valera, 2021). Other studies proposed architectural solutions, including progressive networks (Rusu et al., 2016), attention-based routing (Ma et al., 2019), and dynamic architecture adaptation (Sun et al., 2020). Another line of works focuses on dynamic loss weighting, with methods like uncertainty weighting (Kendall et al., 2018) and DWA (Liu et al., 2019) automatically balancing task losses based on pre-defined criteria. In the related field of continual learning, Zeng et al. (2019) proposed a method that enforces orthogonality between gradient vectors to address the issue of catastrophic forgetting.

These advances in handling conflicting gradients provide valuable insights for machine unlearning, where the goal is to satisfy both the unlearning objective and maintain performance on retained data.

In this work, we focus on evaluating machine unlearning across various setups in the contexts of image classification and Automatic Speech Recognition (ASR). By exploring different unlearning scenarios, we aim to test the generalization capabilities of all methods, particularly in handling large-scale datasets and scenarios with restricted access to the original training data.

Algorithm 1 OrthoGrad

Input: Forget set \mathcal{D}_u , retain set \mathcal{D}_r , learning rate η , combination parameter α

Output: Updated model parameters θ_p

Apply LoRA modules to the pretrained model:

$$\theta_l = LoRA(\theta_p)$$

repeat

 Sample a batch $\mathcal{B}_u \subset \mathcal{D}_u$ and $\mathcal{B}_r \subset \mathcal{D}_r$

 Compute the gradient g_u from \mathcal{B}_u

 Compute the retain batch per-sample gradient matrix:

$$G_r = [g_r^1, g_r^2, \dots, g_r^k] \text{ from } \mathcal{B}_r$$

 Perform QR decomposition on G_r to extract subspace:

$$Q = QR(G_r), \quad Q = [q_r^1, q_r^2, \dots, q_r^k]$$

 Project g_u onto the retain gradient subspace:

$$p_i = \langle g_u, q_r^i \rangle q_r^i$$

 Compute the orthogonalized unlearn gradient:

$$g_u^{\perp} = g_u - \sum_{j=1}^k p_j$$

 Compute the mean retain gradient:

$$\bar{g}_r = \frac{1}{k} \sum_{j=1}^k g_r^j$$

 Combine gradients to form a unified update direction:

$$g = \alpha \bar{g}_r + (1 - \alpha) g_u^{\perp}$$

 Update model parameters:

$$\theta_l \leftarrow \theta_l - \eta g$$

until Convergence or maximum number of iterations

Merge LoRA modules:

$$\theta_p = Merge(\theta_p, \theta_l)$$

3. Background

We consider a training dataset $\mathcal{D} = \{(x_i, y_i)\}_{i=1}^N$ with each data point representing a pair of input vector x_i and its corresponding label y_i . A machine learning model $f(\cdot; \theta)$, parameterized by parameters θ , is optimized to minimize a loss function $\mathcal{L}(\theta)$. Formally we define the loss function as $\mathcal{L}(\theta) = \frac{1}{N} \sum_{i=1}^N \ell(f(x_i; \theta), y_i)$, where ℓ is the cross entropy loss. The model parameters trained on \mathcal{D} are denoted as θ_p representing the *pretrained model*. In machine unlearning, we are given two datasets: (i) Unlearn set $\mathcal{D}_u = \{(x_i, y_i)\}_{i=1}^{N_u}$, containing the N_u data points to be unlearned. (ii) Retain set $\mathcal{D}_r = \{(x_i, y_i)\}_{i=1}^{N_r}$, with N_r samples representing the training data to aid retain the model’s performance. We assume these two datasets are disjoint, i.e., $\mathcal{D}_u \cap \mathcal{D}_r = \emptyset$. The primary goal of machine unlearning is to modify the model’s weights to obtain θ_u resulting in an *unlearned model* $f(\cdot; \theta_u)$. This modification process aims to remove the knowledge of the original model of \mathcal{D}_u . At the same time, the model must maintain its predictive performance on unseen data.

One major challenge in machine unlearning is how to define if the unlearn set was successfully unlearned. While theoretically, we want our model to be indistinguishable from a model trained from scratch without the unlearn set, this

Table 2. Automatic Speech Recognition. ASR speaker unlearning results on LibriSpeech dataset. Word error rate values are averaged over 5 different speakers.

Method	\mathcal{W}_{retain}	$\mathcal{W}_{unlearn}$	$\mathcal{W}_{speaker}$	\mathcal{W}_{test}
Original	9.99 ± 0.15	11.12 ± 4.91	10.06 ± 6.39	11.08 ± 0.00
Finetune	0.06 ± 0.01	13.39 ± 5.26	12.54 ± 7.48	13.67 ± 0.04
NegGrad+	72.87 ± 19.18	77.08 ± 35.99	94.89 ± 6.78	85.90 ± 10.72
SCRUB	100.00 ± 0.00	100.00 ± 0.00	100.00 ± 0.00	100.00 ± 0.00
GDR-GMA	17.38 ± 9.69	93.28 ± 7.58	94.76 ± 6.23	32.52 ± 5.72
OrthoGrad	12.11 ± 0.65	96.24 ± 8.06	98.53 ± 3.28	13.98 ± 0.58

is hard to verify without actually retraining from scratch. In this work, similar to Cotogni et al. (2023), we aim for the performance on the unlearn set to match the original models’ performance on the test set as a proxy. This also has the added benefit of making the comparison between different unlearning methods straightforward. As we care about both unlearn set performance and test set performance, by normalizing the unlearn set performance of all models (up to some tolerance) we can directly compare using a single metric, i.e., the test set performance.

4. Method

In this section, we introduce OrthoGrad, a novel approach to machine unlearning that is designed to address two key challenges in machine unlearning: conflicting gradients and unlearning with a limited amount of retain data. We observe that current unlearning methods rely heavily on the retain set. Some methods (Cotogni et al., 2023), even designed a second phase where they train on the retain set to improve test performance. While this can be a valid approach, it inherently assumes that one has access to a large retain set that represents the full training data faithfully. In many cases, models are made publicly available but their training data is proprietary. It is however reasonable to assume we have access to some small publicly available retain set representing a portion of the train set.

We argue that the reliance on both gradient ascent for unlearning and gradient descent for retention contributes to the excessive dependence on the retain set. In a sense, we are simultaneously forgetting and retraining during the unlearning phase. Considering this, our main guideline in designing our approach is to mitigate the negative effect of the unlearning step instead of fixing it using the retain set.

4.1. Geometric Motivation

Intuitively, we are interested in the set of parameter vectors $\theta \in \mathbb{R}^d$ that maintains a constant loss over the retain set \mathcal{D}_r . Formally, let $\tilde{\mathcal{L}}_r(\theta) = (\ell_1(\theta), \dots, \ell_{N_r}(\theta))$ define the vector of losses over the retain set, we are interested in

performing unlearning in the level set $\bar{\Theta} := \{\theta \in \mathbb{R}^d \mid \tilde{\mathcal{L}}_r(\theta) = \tilde{\mathcal{L}}_r(\theta_p)\}$, i.e., unlearning without changing the loss on our retain set.

Claim 1. *Assuming that (i) The loss ℓ is continuously differentiable, and (ii) The Jacobian of the retain loss $\nabla \tilde{\mathcal{L}} \in \mathbb{R}^{n \times d}$ is of full rank for all $\theta \in \bar{\Theta}$ then $\bar{\Theta}$ is a smooth manifold of dimension $d - N_r$.*

Proof Sketch. To see that, we define for $\theta' \in \bar{\Theta}$ the function $f : \mathbb{R}^d \rightarrow \mathbb{R}^n$ by $f(\theta) = \tilde{\mathcal{L}}_r(\theta) - \tilde{\mathcal{L}}_r(\theta_p)$. From our assumptions, f is continuously differentiable, and the Jacobian of f , $\nabla f = \nabla \tilde{\mathcal{L}}_r$ has full rank at θ' . Thus, as a direct result of the implicit function theorem, the set $\bar{\Theta}$ is locally diffeomorphic to an open ball in \mathbb{R}^{d-N_r} . \square

If we consider our optimization as a discretization of a gradient flow, it would be natural to look at the gradient flow on the $\bar{\Theta}$ manifold. To do that we would need to first project our gradient to the tangent space.

Claim 2. *The tangent space $T_{\theta'}\bar{\Theta}$ to $\bar{\Theta}$ at θ' is given by the null space of the Jacobian $\nabla_{\theta'}\tilde{\mathcal{L}}_r$, that is, the set of directions in parameter space that are orthogonal to the subspace spanned by the retain gradients, $T_{\theta'}\bar{\Theta} = \{v \in \mathbb{R}^d \mid \nabla \tilde{\mathcal{L}}_r v = 0\}$*

Proof Sketch. To show that $T_{\theta'}\bar{\Theta} = \text{Ker}(\nabla_{\theta'}\tilde{\mathcal{L}}_r)$, we first note that $T_{\theta'}\bar{\Theta} \subset \text{Ker}(\nabla_{\theta'}\tilde{\mathcal{L}}_r)$: Let $v \in T_{\theta'}\bar{\Theta}$ and let $\gamma(\cdot)$ be a smooth curve in $\bar{\Theta}$ with $\gamma(0) = \theta'$ and $\dot{\gamma}(0) = v$, we have $0 = \frac{d}{dt}f(\gamma(t)) \big|_{t=0} = \nabla_{\theta'}\tilde{\mathcal{L}}_r v$, and so $v \in \text{Ker}(\nabla_{\theta'}\tilde{\mathcal{L}}_r)$. Finally, we get the equality $T_{\theta'}\bar{\Theta} = \text{Ker}(\nabla_{\theta'}\tilde{\mathcal{L}}_r)$ following a dimension counting argument since $\dim(T_{\theta'}\bar{\Theta}) = \dim(\text{Ker}(\nabla_{\theta'}\tilde{\mathcal{L}}_r)) = d - N_r$. \square

While it is possible to try and solve the manifold flow for unlearning, it is too computationally demanding in practice. This would require to first compute and store the gradients on the entire retain set. Even with our assumption of a relatively small retain set this can still be expensive and require a significant amount of GPU memory. Second, using discrete gradient updates will cause our solutions to drift from that manifold and will involve an expensive step projecting them back to $\bar{\Theta}$.

Table 3. *ImageNet with ViT architecture*. Performance is measured under two unlearning scenarios: random sampling of training data (left side, 3-seed average) and complete class removal (right side, 3-class average).

Method	Random Sampling				Class Forgetting			
	\mathcal{A}_u	\mathcal{A}_r	\mathcal{A}_{test}	UIS (\downarrow)	\mathcal{A}_u	\mathcal{A}_r	\mathcal{A}_{test}	UIS (\downarrow)
Original	94.26 \pm 0.19	94.04 \pm 0.24	81.06 \pm 0.00	–	98.1 \pm 1.62	94.17 \pm 0.00	81.06 \pm 0.00	–
FT	89.96 \pm 0.56	99.94 \pm 0.01	75.03 \pm 0.30	–	91.97 \pm 8.18	99.92 \pm 0.02	74.07 \pm 0.05	–
NegGrad	24.2 \pm 13.23	24.26 \pm 13.46	21.06 \pm 14.06	0.720 \pm 0.186	0.41 \pm 0.34	89.63 \pm 3.84	76.53 \pm 4.16	0.030 \pm 0.028
NegGrad+	78.75 \pm 3.09	87.63 \pm 5.34	72.16 \pm 4.53	0.069 \pm 0.051	0.05 \pm 0.07	90.67 \pm 4.22	77.17 \pm 4.73	0.024 \pm 0.028
FISHER	94.36 \pm 0.09	94.01 \pm 0.19	81.00 \pm 0.05	0.082 \pm 0.000	98.02 \pm 1.82	94.14 \pm 0.00	80.99 \pm 0.00	0.605 \pm 0.011
Influence	89.08 \pm 1.90	91.61 \pm 1.78	77.48 \pm 1.68	0.071 \pm 0.001	15.28 \pm 20.76	91.54 \pm 2.21	78.13 \pm 2.06	0.112 \pm 0.121
SCRUB	94.54 \pm 0.15	96.00 \pm 0.11	80.76 \pm 0.05	0.084 \pm 0.001	45.82 \pm 37.8	96.18 \pm 2.91	75.81 \pm 4.13	0.314 \pm 0.286
DUCK	76.75 \pm 0.47	100.00 \pm 0.00	69.45 \pm 0.49	0.097 \pm 0.000	0.00 \pm 0.00	99.39 \pm 0.02	70.68 \pm 0.29	0.064 \pm 0.001
GDR-GMA	80.41 \pm 0.34	99.34 \pm 0.05	75.47 \pm 0.16	0.038 \pm 0.003	0.15 \pm 0.16	97.56 \pm 0.18	77.03 \pm 0.28	0.025 \pm 0.001
OrthoGrad	81.04 \pm 0.13	97.59 \pm 0.11	78.22 \pm 0.13	0.018 \pm 0.001	0.10 \pm 0.14	94.26 \pm 0.04	80.73 \pm 0.05	0.002 \pm 0.000

4.2. Practical Algorithm

While performing the exact gradient flow on the retain set it is computationally expensive to run in practice, it inspires the design of our simple and practical unlearning algorithm OrthoGrad. At each optimization step, we simply project the unlearn gradient to the space orthogonal to all individual gradients of the retain set.

Specifically, at each step, we sample a batch of examples from the unlearn set \mathcal{D}_u and calculate the mean gradient vector on this batch. We denote this gradient vector as g_u . Next, we sample a batch from the retain set \mathcal{D}_r . For the retain batch with k samples, we compute the per-sample gradient matrix $G_r = [g_r^1, g_r^2, \dots, g_r^k]$, where each column g_r^i corresponds to the gradient vector for sample i in the batch. Importantly, we note that this can be achieved efficiently using modern automatic differentiation libraries, such as PyTorch (Paszke et al., 2019), which allow us to obtain per-sample gradients in a single forward-backward pass.

To ensure orthogonality between g_u and the column space of G_r we employ QR decomposition (Francis, 1961) on G_r . This yields an orthonormal basis $Q = [q_r^1, q_r^2, \dots, q_r^k]$ that spans this subspace. Once the retain gradient subspace is defined, we project the unlearn gradient onto this subspace to compute its projection w.r.t each subspace vector. For a single retain gradient g_r^i , the projection is calculated as: $g_u^\perp = g_u - \sum_{j=1}^k \langle g_u, q_r^j \rangle q_r^j$. We note that while previous algorithms, for example Lin et al. (2024), do try to mitigate interference between the unlearn and the retain set gradients, they achieve this on the batch-level average gradients and not on the gradients of the individual data points. We found in our experiments that the more strict per-element constraint, instead of working on the mean gradient gives a stronger performance (Section 5.1.1).

To further improve our method we perform two additional modifications. First, we do not change the entire weight space but use low-rank adaptation (LoRA) (Hu et al., 2021)

to further limit the effect that our unlearning has on the overall test performance. We note that in general parameter efficient fine-tuning (PEFT) is a rapidly evolving field and how to best utilize it for unlearning have yet to be thoroughly explored. Finally, we observed that while we are not over-reliant on the retain set, we might in fact be under-utilizing it, thus leading to sub-optimal results. We observe that linearly combining the retain and unlearn gradients yields better results. This approach improves the performance of the unlearned model compared to solely performing gradient ascent in the direction of the unlearn gradient. Therefore, we define the update gradient as: $g = \alpha \bar{g}_r + (1 - \alpha)g_u$ where $\bar{g}_r = \frac{1}{k} \sum_{j=1}^k g_r^j$ is the retain gradient averaged over the batch, and $\alpha \in [0, 1]$ is a hyperparameter that controls the trade-off between forgetting and retaining. Finally, we update the model parameters θ using the update rule: $\theta_l \leftarrow \theta_l - \eta g$. The step-by-step procedure of OrthoGrad is presented in Algorithm 1.

In summary, OrthoGrad enforces orthogonality between the unlearn and retain gradients, minimizing the interference between the updates of the forget and retain sets. We found that OrthoGrad is particularly effective in low-data regimes, due to its limited reliance on the retain set. We demonstrate OrthoGrad effectiveness on various dataset and model architectures in the next section.

5. Experiments

In this section, we compare OrthoGrad with recent approaches for machine unlearning. We use several datasets, model architectures, and unlearning setups to demonstrate the effectiveness and versatility of OrthoGrad in a low data regime, i.e., considering a limited number of retain data points. To encourage future research and reproducibility, we will make our code publicly available. Additional experimental results and details are provided in Appendix A.

Table 4. ImageNet using ResNet18. Results are shown for two scenarios: random sampling (averaged over 3 seeds) and class forgetting (averaged over 3 classes).

Method	Random Sampling				Class Forgetting			
	\mathcal{A}_u	\mathcal{A}_r	\mathcal{A}_{test}	UIS (\downarrow)	\mathcal{A}_u	\mathcal{A}_r	\mathcal{A}_{test}	UIS (\downarrow)
Original	79.04 \pm 0.68	79.2 \pm 0.49	69.76 \pm 0.00	–	91.76 \pm 4.79	79.15 \pm 0.00	69.76 \pm 0.00	–
FT	76.81 \pm 0.83	94.59 \pm 0.08	67.85 \pm 0.03	–	78.02 \pm 18.48	94.28 \pm 0.03	67.39 \pm 0.03	–
NegGrad	69.94 \pm 0.14	70.43 \pm 1.52	62.5 \pm 0.70	0.053 \pm 0.003	22.53 \pm 16.39	74.81 \pm 2.09	66.11 \pm 2.12	0.187 \pm 0.129
NegGrad+	78.98 \pm 0.56	79.23 \pm 0.37	69.74 \pm 0.00	0.066 \pm 0.004	28.92 \pm 21.62	75.94 \pm 1.72	67.1 \pm 1.78	0.226 \pm 0.177
FISHER	78.85 \pm 0.70	78.96 \pm 0.44	69.59 \pm 0.09	0.066 \pm 0.005	91.64 \pm 4.87	79.03 \pm 0.00	69.64 \pm 0.00	0.657 \pm 0.034
Influence	78.98 \pm 0.68	79.22 \pm 0.45	69.74 \pm 0.02	0.066 \pm 0.004	78.82 \pm 18.09	78.90 \pm 0.17	69.52 \pm 0.12	0.566 \pm 0.128
SCRUB	78.86 \pm 0.70	84.03 \pm 0.48	69.47 \pm 0.11	0.067 \pm 0.006	0.53 \pm 0.55	83.61 \pm 0.01	69.42 \pm 0.09	0.006 \pm 0.004
DUCK	67.22 \pm 1.29	99.88 \pm 0.00	61.87 \pm 0.01	0.074 \pm 0.011	0.00 \pm 0.00	99.94 \pm 0.00	61.37 \pm 0.74	0.060 \pm 0.006
GDR-GMA	67.35 \pm 1.32	99.97 \pm 0.02	66.98 \pm 0.38	0.037 \pm 0.011	0.74 \pm 0.29	99.22 \pm 0.22	64.74 \pm 0.38	0.043 \pm 0.000
OrthoGrad	69.95 \pm 0.15	82.27 \pm 0.87	67.59 \pm 0.48	0.016 \pm 0.002	0.48 \pm 0.40	77.24 \pm 1.22	67.25 \pm 1.24	0.021 \pm 0.005

Baselines. We compare OrthoGrad with natural baselines from recent machine unlearning works. The compared methods include: (1) Finetune - finetune the pretrained model solely with the retain set. (2) NegGrad (Graves et al., 2021; Thudi et al., 2022) - a naive approach that performs gradient accent steps on the unlearn set. (3) NegGrad+ (Kurmanji et al., 2024) - NegGrad with the additional goal of minimizing retain loss and preserving the model’s knowledge on the retain dataset. (4) FISHER (Golatkar et al., 2020a) - adds additive noise to the pretrained weights with a constraint on the fisher information matrix to maintain the model’s performance on the retain set. (5) Influence (Koh & Liang, 2017; Izzo et al., 2021) - utilizes influence functions to identify the parameters most critical to the data being unlearned and perturb them by adding additive noise. (6) SCRUB (Kurmanji et al., 2024) - A knowledge distillation approach that incorporates a regularization term into the unlearning objective by aligning the pretrained parameters with the unlearning parameters. (7) DUCK (Cotogni et al., 2023) - uses metric learning to minimize the distance between feature vectors of the data to be forgotten and the nearest centroid of a different class. (8) GDR-GMA (Lin et al., 2024) - projecting conflicting gradients onto an orthonormal plane and dynamically adjusting the magnitude of update gradients to balance tasks of unlearn dataset and maintaining the retain dataset.

Evaluation. We report the common evaluation metrics in machine unlearning. Specifically, we evaluate the methods’ performance using two main accuracy metrics: unlearning accuracy (\mathcal{A}_u) on the data to be forgotten, and test accuracy (\mathcal{A}_{test}) on the held-out test set. For completeness, we also report retain accuracy (\mathcal{A}_r) on the retain data, which is comparable to train accuracy in standard learning and should not be used for comparison. In all experiments, we perform early stopping based on \mathcal{A}_u reaching a specific target (normally the original test accuracy). This allows for easier comparison as the main difference is in \mathcal{A}_{test} . Stopping criteria are crucial in machine unlearning to ensure the process reaches a proper balance between effective forgetting with

retained functionality.

As machine unlearning involves multiple objectives, we propose the Unlearning Impact Score (UIS) for easier comparison. Our metric is defined as:

$$UIS = \left(\frac{|\mathcal{A}_{test}^p - \mathcal{A}_{test}^u|}{\mathcal{A}_{test}^p} + \frac{|\mathcal{A}_{test}^p - \mathcal{A}_u^p|}{\mathcal{A}_{test}^p} \right) / 2 \quad ,$$

where the up scripts p and u denote pretrained and unlearned models respectively. In UIS we average two components: the relative change in test accuracy, and how close the performance on the unlearning set is to its target, \mathcal{A}_{test}^p . A lower UIS score indicates better unlearning, as it suggests the model has successfully forgotten the unlearn data while maintaining its performance on held-out data.

5.1. Automatic Speech Recognition

Automatic Speech Recognition (ASR) is the process of converting spoken language into written text, a fundamental component in many real-world applications (Malik et al., 2021; Alharbi et al., 2021). ASR foundation models like Whisper (Radford et al., 2023) are trained on extensive datasets of transcribed web audio containing many hours of speech recordings. Therefore, these models may inadvertently retain sensitive or proprietary information raising legal issues. Furthermore, individuals may wish to ensure that an ASR system cannot accurately transcribe their voice as a way to preserve their privacy. To the best of our knowledge, this is the first unlearning work to evaluate unlearning in such a realistic and challenging setting as ASR.

In this section, we focus on speaker unlearning, the task of forgetting audio data associated with a particular speaker, making this speaker unrecognizable by the ASR system. For our experiments, we utilize Whisper-Tiny (Radford et al., 2023) and the LibriSpeech (Panayotov et al., 2015) dataset, containing 1,000 hours of English speech recordings. We establish the unlearning setup by selecting a single speaker from the training set to serve as the unlearn set. We ran-

Table 5. *CIFAR10* with *ResNet18* architecture. Performance is measured under two unlearning scenarios: random sampling of training data (3-seed average) and complete class removal (3-class average).

Method	Random Sampling				Class Forgetting			
	\mathcal{A}_u	\mathcal{A}_r	\mathcal{A}_{test}	UIS (\downarrow)	\mathcal{A}_u	\mathcal{A}_r	\mathcal{A}_{test}	UIS (\downarrow)
Original	96.1 \pm 0.28	96.38 \pm 0.33	81.97 \pm 0.00	—	97.3 \pm 1.21	95.91 \pm 0.22	81.97 \pm —	—
FT	85.94 \pm 6.34	88.49 \pm 7.44	71.52 \pm 6.61	—	93.79 \pm 2.36	100.00 \pm 0.00	82.86 \pm 0.18	—
NegGrad	40.39 \pm 22.59	39.78 \pm 23.17	34.94 \pm 22.87	0.54 \pm 0.308	0.00 \pm 0.00	18.72 \pm 10.03	15.43 \pm 9.40	0.405 \pm 0.057
NegGrad+	81.42 \pm 0.63	83.00 \pm 0.59	69.25 \pm 1.08	0.082 \pm 0.009	24.54 \pm 33.85	70.56 \pm 25.45	56.42 \pm 24.31	0.305 \pm 0.164
FISHER	72.29 \pm 6.59	72.57 \pm 6.55	61.60 \pm 6.75	0.183 \pm 0.089	84.98 \pm 21.79	69.08 \pm 5.77	61.33 \pm 1.92	0.645 \pm 0.143
Influence	11.55 \pm 1.42	11.59 \pm 1.30	11.31 \pm 1.48	0.860 \pm 0.019	43.07 \pm 29.16	66.72 \pm 31.99	54.53 \pm 25.95	0.431 \pm 0.043
SCRUB	40.18 \pm 5.37	42.51 \pm 4.88	38.58 \pm 4.30	0.519 \pm 0.066	1.75 \pm 1.61	87.32 \pm 3.09	64.7 \pm 1.70	0.116 \pm 0.022
DUCK	86.46 \pm 0.19	99.5 \pm 0.29	78.02 \pm 0.35	0.051 \pm 0.002	0.00 \pm 0.00	41.28 \pm 4.25	35.35 \pm 4.82	0.284 \pm 0.029
GDR-GMA	81.75 \pm 0.40	99.08 \pm 0.41	71.6 \pm 0.28	0.065 \pm 0.002	0.19 \pm 0.19	89.88 \pm 5.31	66.79 \pm 3.30	0.093 \pm 0.021
OrthoGrad	81.18 \pm 2.92	93.27 \pm 0.71	73.35 \pm 0.41	0.058 \pm 0.005	0.36 \pm 0.35	97.57 \pm 0.43	74.87 \pm 1.05	0.045 \pm 0.006

domly allocate 10% from the unlearn set to evaluate our model on the unlearned speaker. Additionally, we randomly sample 10% of the remaining training set to form the retain set. The test set is taken directly from the original LibriSpeech.

We evaluate the performance using the word error rate (WER), a standard metric that measures the percentage of words incorrectly transcribed by the model. We report WER for the unlearn (\mathcal{W}_u), retain (\mathcal{W}_r), test (\mathcal{W}_{test}), and speaker held out ($\mathcal{W}_{speaker}$) datasets. The speaker held-out dataset comprise of unseen audio recordings that belong the the unlearned speaker. Since Whisper model tends to hallucinate (Koenecke et al., 2024) by predicting unwanted words, we clip the WER at a maximum of 100%.

5.1.1. ABLATION STUDY

We begin with an ablation study to evaluate the relative contribution of each component in our approach. We run the unlearning process for 30 epochs with an early stopping when \mathcal{W}_u reaches 75%. We note that the WER tends to jump significantly during the last epochs which can lead to a final WER that is much higher than our stopping criteria. Although the exact threshold is somewhat arbitrary, we observed a rapid increase in WER beyond a certain point. This suggests that the results should remain robust regardless of the specific threshold chosen. In this experiment we compare (i) OrthoGrad Mean; Projecting the unlearn gradient to be orthogonal to the average retain gradient (ii) OrthoGrad Per-sample; Projecting the unlearn gradient to the space orthogonal to all individual sample gradients (iii) OrthoGrad Mean/Per-sample+LoRA; The previous methods when the update is restricted to low-rank adaptors. (iv) OrthoGrad; Our full method that combines gradient descent on the retain set. The results, averaged over 5 speakers, are presented in Table 1.

We first note that using the per-sample orthogonalization has two benefits. It not only reduces the mean \mathcal{W}_{test} , but

also reduces the variance by an order of magnitude. We observed that OrthoGrad Mean is very unstable and while it can work well on some speakers it performs poorly on others. Next, we note that restricting the OrthoGrad per-sample unlearning to LoRA adaptors offers a significant improvement in \mathcal{W}_{test} . However, this is not the case for OrthoGrad Mean due to instability. In addition, we note that while all methods passed the 75% WER threshold on the unlearn set with a large margin, the OrthoGrad Mean performance on unseen audio from the speaker, $\mathcal{W}_{speaker}$ was below our target threshold. This means the unlearning did not generalize as well to new recordings of the unlearned speaker. Finally, we see that adding the retain gradient can offer an additional improvement, but this improvement is somewhat limited.

5.1.2. ASR RESULTS

Next, we compare our OrthoGrad method to leading machine unlearning approaches. We compare OrthoGrad to SCRUB (Kurmanji et al., 2024), GDR-GMA (Lin et al., 2024), and NegGrad+ (Kurmanji et al., 2024). We exclude DUCK (Cotogni et al., 2023) as it is designed for classification and is unsuitable for ASR. The technical details and hyperparameter selection are provided in Appendix A.2.

The results are shown in Table 2. All methods, except for the finetune baseline, successfully unlearned the target speaker. We hypothesize that the high \mathcal{W}_{test} values for both NegGrad+ and SCRUB (Kurmanji et al., 2024) arise from the fact they do not take into account the conflict between the unlearn and retain gradients. In contrast, OrthoGrad and GDR-GMA which consider this conflict, work well on this benchmark. Moreover, our approach outperforms GDR-GMA by maintaining significantly better performance on the test set.

5.2. Image Classification

Image classification tasks are commonly used benchmarks for evaluating machine unlearning algorithms. These benchmarks have two variations: class-wise forgetting and random data forgetting. Class-wise forgetting focuses on removing the influence of an entire image class, while random data forgetting targets the removal of randomly selected data points from the training set. In the standard experimental setup the entire training set, except for the unlearn set, is used as the retain set. We, however, are interested in the scenario where we have access to a limited retain set, and therefore subsample a portion of the training set to be our retain set.

Our evaluation is conducted on two image classification datasets: CIFAR10 (Krizhevsky et al., 2009) and ImageNet (Deng et al., 2009). We sample 5K and 10K images as the retain set for CIFAR10 and ImageNet respectively. We utilize the original test set in both cases. We use ResNet-18 (He et al., 2016) for both datasets and additionally use ViT (Dosovitskiy, 2020) for ImageNet (Deng et al., 2009) as our base classifiers.

The stopping criteria used in the random forgetting experiments follows Cotogni et al. (2023) - we stop when the unlearn accuracy is within a defined threshold (0.5) or lower than the test accuracy of the pretrained model. For class-wise forgetting, we stopped when the model’s accuracy on the unlearned classes dropped below 1%, indicating that the class had been effectively forgotten. In both cases, if the unlearning algorithm does not reach the target within a specific number of epochs, we report the results of the last epoch.

The results in Tables 3 and 4 provide a comprehensive evaluation of machine unlearning methods on ImageNet using ViT and ResNet18 architectures, respectively. These experiments show that our method reliably reaches the target unlearn value and achieves the best test performance in all experiments besides class forgetting on ResNet18 where it is second to SCRUB. Interestingly, we note that while SCRUB performs exceptionally well in class forgetting with ResNet18, it performs poorly in other experimental setups.

We present additional results on CIFAR-10 dataset using ResNet18 architecture in Table 5. In these experiments, OrthoGrad again reaches the unlearn target with excellent test performance. While DUCK has overall better test performance and UIS score in the random sampling experiment, it failed to reach the unlearn target value by a large margin.

5.2.1. ROBUSTNESS TO RETAIN SIZE

In this work, we experiment with small-sized retain sets. Here, we wish to assess the robustness of our method to variations in the retain set size. To do so, we revisit the ran-

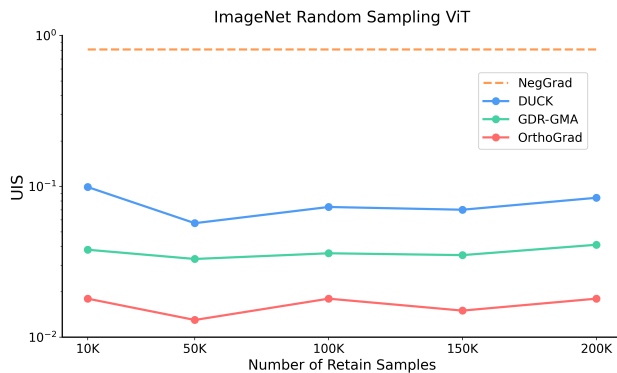


Figure 2. Performance comparison of different gradient-based methods on ImageNet with ViT architecture. We report UIS values across varying numbers of retained samples.

dom sampling image classification setup from Section 5.2. Specifically, we experiment with varying retain dataset sizes, ranging from 10K to 200K samples, reporting the UIS values.

The results are presented in Figure 2, with additional robustness results in the appendix (Figure 3). We note that NegGrad is not affected by the size of the retain set since it only performs gradient accent in the direction of the unlearn set. Our model consistently outperforms baseline methods across all retain set sizes.

6. Limitations

This work focuses on the low-data regime and demonstrates significant improvements over competing methods in this setting. However, its performance may not scale as effectively when the full retain dataset is available. Additionally, the per-sample gradient manipulations required for retain data introduce higher GPU memory demands compared to other unlearning methods. Despite these limitations, OrthoGrad presents a compelling solution in data-constrained environments.

7. Conclusions

In this work, we focus on machine unlearning in the low data regime, where access to the retain data is limited. We present OrthoGrad, a novel machine unlearning method that reduces reliance on the retain set. We achieve this by projecting the aggregated unlearn gradient onto the subspace orthogonal to the individual gradients of the retain batch. First, we provide a geometric motivation for our projection approach. Next, in an ablation study, we show the benefit of considering the per-sample gradient in the retain batch. Finally, we demonstrate through various datasets,

architectures, and unlearning setups the superiority of OrthoGrad over existing machine unlearning methods. The reduced dependency of OrthoGrad in large retain set, makes it a practical solution for real-life applications where data availability is constrained by privacy concerns.

8. Acknowledgments

This research was supported by the Israeli Ministry of Science, Israel-Singapore binational grants 207606 and 207627.

References

- Alharbi, S., Alrazgan, M., Alrashed, A., Alnomasi, T., Almojel, R., Alharbi, R., Alharbi, S., Alturki, S., Alshehri, F., and Almojil, M. Automatic speech recognition: Systematic literature review. *Ieee Access*, 9:131858–131876, 2021.
- Becker, A. and Liebig, T. Evaluating machine unlearning via epistemic uncertainty. *arXiv preprint arXiv:2208.10836*, 2022.
- Brown, T., Mann, B., Ryder, N., Subbiah, M., Kaplan, J. D., Dhariwal, P., Neelakantan, A., Shyam, P., Sastry, G., Askell, A., et al. Language models are few-shot learners. *Advances in neural information processing systems*, 33: 1877–1901, 2020.
- Cao, Y. and Yang, J. Towards making systems forget with machine unlearning. In *2015 IEEE symposium on security and privacy*, pp. 463–480. IEEE, 2015.
- Carlini, N., Tramer, F., Wallace, E., Jagielski, M., Herbert-Voss, A., Lee, K., Roberts, A., Brown, T., Song, D., Erlingsson, U., et al. Extracting training data from large language models. In *30th USENIX Security Symposium (USENIX Security 21)*, 2021.
- Chen, M., Zhang, Z., Wang, T., Backes, M., Humbert, M., and Zhang, Y. Graph unlearning. In *Proceedings of the 2022 ACM SIGSAC conference on computer and communications security*, pp. 499–513, 2022.
- Chen, M., Gao, W., Liu, G., Peng, K., and Wang, C. Boundary unlearning: Rapid forgetting of deep networks via shifting the decision boundary. In *Proceedings of the IEEE/CVF Conference on Computer Vision and Pattern Recognition*, pp. 7766–7775, 2023.
- Chen, Z., Badrinarayanan, V., Lee, C.-Y., and Rabinovich, A. Gradnorm: Gradient normalization for adaptive loss balancing in deep multitask networks. In *International conference on machine learning*, pp. 794–803. PMLR, 2018.
- Chen, Z., Badrinarayanan, V., Lee, C.-Y., and Rabinovich, A. Just pick a sign: Optimizing deep multitask models with gradient sign dropout. In *Advances in Neural Information Processing Systems*, volume 33, pp. 19834–19845, 2020.
- Cheng, J., Dasoulas, G., He, H., Agarwal, C., and Zitnik, M. Gnndelete: A general strategy for unlearning in graph neural networks. *arXiv preprint arXiv:2302.13406*, 2023.
- Cotogni, M., Bonato, J., Sabetta, L., Pelosin, F., and Nicolosi, A. Duck: Distance-based unlearning via centroid kinematics. *arXiv preprint arXiv:2312.02052*, 2023.
- Crawshaw, M. Multi-task learning with deep neural networks: A survey. *arXiv preprint arXiv:2009.09796*, 2020.
- Dakhel, A. M., Majdinasab, V., Nikanjam, A., Khomh, F., Desmarais, M. C., and Jiang, Z. M. J. Github copilot ai pair programmer: Asset or liability? *Journal of Systems and Software*, 203:111734, 2023.
- Deng, J., Dong, W., Socher, R., Li, L.-J., Li, K., and Fei-Fei, L. Imagenet: A large-scale hierarchical image database. In *2009 IEEE conference on computer vision and pattern recognition*, pp. 248–255. Ieee, 2009.
- Dosovitskiy, A. An image is worth 16x16 words: Transformers for image recognition at scale. *arXiv preprint arXiv:2010.11929*, 2020.
- Dwork, C., Kenthapadi, K., McSherry, F., Mironov, I., and Naor, M. Our data, ourselves: Privacy via distributed noise generation. In *Advances in Cryptology-EUROCRYPT 2006: 24th Annual International Conference on the Theory and Applications of Cryptographic Techniques, St. Petersburg, Russia, May 28-June 1, 2006. Proceedings 25*, pp. 486–503. Springer, 2006.
- Fan, C., Liu, J., Zhang, Y., Wong, E., Wei, D., and Liu, S. Salun: Empowering machine unlearning via gradient-based weight saliency in both image classification and generation. *arXiv preprint arXiv:2310.12508*, 2023.
- Fan, C., Liu, J., Hero, A., and Liu, S. Challenging forgets: Unveiling the worst-case forget sets in machine unlearning. In *European Conference on Computer Vision*, pp. 278–297. Springer, 2025.
- Francis, J. G. The qr transformation a unitary analogue to the lr transformation—part 1. *The Computer Journal*, 4 (3):265–271, 1961.
- Ginart, A., Guan, M., Valiant, G., and Zou, J. Y. Making ai forget you: Data deletion in machine learning. *Advances in neural information processing systems*, 32, 2019.
- Goel, S., Prabhu, A., Sanyal, A., Lim, S.-N., Torr, P., and Kumaraguru, P. Towards adversarial evaluations for inexact

- machine unlearning. *arXiv preprint arXiv:2201.06640*, 2022.
- Golatkar, A., Achille, A., and Soatto, S. Eternal sunshine of the spotless net: Selective forgetting in deep networks. In *Proceedings of the IEEE/CVF Conference on Computer Vision and Pattern Recognition*, pp. 9304–9312, 2020a.
- Golatkar, A., Achille, A., and Soatto, S. Forgetting outside the box: Scrubbing deep networks of information accessible from input-output observations. In *Computer Vision—ECCV 2020: 16th European Conference, Glasgow, UK, August 23–28, 2020, Proceedings, Part XXIX 16*, pp. 383–398. Springer, 2020b.
- Golatkar, A., Achille, A., Ravichandran, A., Polito, M., and Soatto, S. Mixed-privacy forgetting in deep networks. In *Proceedings of the IEEE/CVF conference on computer vision and pattern recognition*, pp. 792–801, 2021.
- Graves, L., Nagisetty, V., and Ganesh, V. Amnesiac machine learning. In *Proceedings of the AAAI Conference on Artificial Intelligence*, volume 35, pp. 11516–11524, 2021.
- Guo, C., Goldstein, T., Hannun, A., and Van Der Maaten, L. Certified data removal from machine learning models. *arXiv preprint arXiv:1911.03030*, 2019.
- He, K., Zhang, X., Ren, S., and Sun, J. Deep residual learning for image recognition. In *Proceedings of the IEEE conference on computer vision and pattern recognition*, pp. 770–778, 2016.
- Hu, J. E., Shen, Y., Wallis, P., Allen-Zhu, Z., Li, Y., Wang, S., and Chen, W. Lora: Low-rank adaptation of large language models. *ArXiv*, abs/2106.09685, 2021. URL <https://api.semanticscholar.org/CorpusID:235458009>.
- Huang, M. H., Foo, L. G., and Liu, J. Learning to unlearn for robust machine unlearning. In *European Conference on Computer Vision*, pp. 202–219. Springer, 2025.
- Izzo, Z., Smart, M. A., Chaudhuri, K., and Zou, J. Approximate data deletion from machine learning models. In *International Conference on Artificial Intelligence and Statistics*, pp. 2008–2016. PMLR, 2021.
- Javaloy, A. and Valera, I. Rotograd: Gradient homogenization in multitask learning. *arXiv preprint arXiv:2103.02631*, 2021.
- Jia, J., Liu, J., Ram, P., Yao, Y., Liu, G., Liu, Y., Sharma, P., and Liu, S. Model sparsification can simplify machine unlearning. *arXiv preprint arXiv:2304.04934*, 1(2):3, 2023.
- Kendall, A., Gal, Y., and Cipolla, R. Multi-task learning using uncertainty to weigh losses for scene geometry and semantics. In *Proceedings of the IEEE Conference on Computer Vision and Pattern Recognition*, pp. 7482–7491, 2018.
- Kingma, D. P. Adam: A method for stochastic optimization. *arXiv preprint arXiv:1412.6980*, 2014.
- Koenecke, A., Choi, A. S. G., Mei, K. X., Schellmann, H., and Sloane, M. Careless whisper: Speech-to-text hallucination harms. In *The 2024 ACM Conference on Fairness, Accountability, and Transparency*, pp. 1672–1681, 2024.
- Koh, P. W. and Liang, P. Understanding black-box predictions via influence functions. In *International conference on machine learning*, pp. 1885–1894. PMLR, 2017.
- Krizhevsky, A., Hinton, G., et al. Learning multiple layers of features from tiny images. 2009.
- Kurmanji, M., Triantafillou, P., Hayes, J., and Triantafillou, E. Towards unbounded machine unlearning. *Advances in neural information processing systems*, 36, 2024.
- Lin, S., Zhang, X., Susilo, W., Chen, X., and Liu, J. Gdr-gma: Machine unlearning via direction-rectified and magnitude-adjusted gradients. In *Proceedings of the 32nd ACM International Conference on Multimedia*, pp. 9087–9095, 2024.
- Liu, B., Liu, X., Jin, X., Stone, P., and Liu, Q. Conflict-averse gradient descent for multi-task learning. *Advances in Neural Information Processing Systems*, 34:18878–18890, 2021a.
- Liu, G., Ma, X., Yang, Y., Wang, C., and Liu, J. Feder-eraser: Enabling efficient client-level data removal from federated learning models. In *2021 IEEE/ACM 29th international symposium on quality of service (IWQoS)*, pp. 1–10. IEEE, 2021b.
- Liu, S., Johns, E., and Davison, A. J. End-to-end multi-task learning with attention. In *Proceedings of the IEEE/CVF Conference on Computer Vision and Pattern Recognition*, pp. 1871–1880, 2019.
- Liu, Y., Xu, L., Yuan, X., Wang, C., and Li, B. The right to be forgotten in federated learning: An efficient realization with rapid retraining. In *IEEE INFOCOM 2022-IEEE Conference on Computer Communications*, pp. 1749–1758. IEEE, 2022.
- Liu, Z., Ye, H., Chen, C., Zheng, Y., and Lam, K.-Y. Threats, attacks, and defenses in machine unlearning: A survey. *arXiv preprint arXiv:2403.13682*, 2024.

- Lopez-Paz, D. and Ranzato, M. Gradient episodic memory for continual learning. *Advances in neural information processing systems*, 30, 2017.
- Ma, J., Zhao, Z., Chen, J., Li, A., Hong, L., and Chi, E. H. Snr: Sub-network routing for flexible parameter sharing in multi-task learning. In *Proceedings of the AAAI conference on artificial intelligence*, volume 33, pp. 216–223, 2019.
- Malik, M., Malik, M. K., Mehmood, K., and Makhdoom, I. Automatic speech recognition: a survey. *Multimedia Tools and Applications*, 80:9411–9457, 2021.
- Mehta, R., Pal, S., Singh, V., and Ravi, S. N. Deep unlearning via randomized conditionally independent Hessians. In *Proceedings of the IEEE/CVF Conference on Computer Vision and Pattern Recognition*, pp. 10422–10431, 2022.
- Navon, A., Shamsian, A., Achituve, I., Maron, H., Kawaguchi, K., Chechik, G., and Fetaya, E. Multi-task learning as a bargaining game. *arXiv preprint arXiv:2202.01017*, 2022.
- Neel, S., Roth, A., and Sharifi-Malvajerdi, S. Descent-to-delete: Gradient-based methods for machine unlearning. In *Algorithmic Learning Theory*, pp. 931–962. PMLR, 2021.
- Nguyen, T. T., Huynh, T. T., Ren, Z., Nguyen, P. L., Liew, A. W.-C., Yin, H., and Nguyen, Q. V. H. A survey of machine unlearning. *arXiv preprint arXiv:2209.02299*, 2022.
- Panayotov, V., Chen, G., Povey, D., and Khudanpur, S. Librispeech: an asr corpus based on public domain audio books. In *2015 IEEE international conference on acoustics, speech and signal processing (ICASSP)*, pp. 5206–5210. IEEE, 2015.
- Paszke, A., Gross, S., Massa, F., Lerer, A., Bradbury, J., Chanan, G., Killeen, T., Lin, Z., Gimelshein, N., Antiga, L., et al. Pytorch: An imperative style, high-performance deep learning library. *Advances in neural information processing systems*, 32, 2019.
- Radford, A., Kim, J. W., Hallacy, C., Ramesh, A., Goh, G., Agarwal, S., Sastry, G., Askell, A., Mishkin, P., Clark, J., et al. Learning transferable visual models from natural language supervision. In *International conference on machine learning*, pp. 8748–8763. PMLR, 2021.
- Radford, A., Kim, J. W., Xu, T., Brockman, G., McLeavey, C., and Sutskever, I. Robust speech recognition via large-scale weak supervision. In *International conference on machine learning*, pp. 28492–28518. PMLR, 2023.
- Romero, E., Barrio, I., and Belanche, L. Incremental and decremental learning for linear support vector machines. In *International Conference on Artificial Neural Networks*, pp. 209–218. Springer, 2007.
- Rusu, A. A., Rabinowitz, N. C., Desjardins, G., Soyer, H., Kirkpatrick, J., Kavukcuoglu, K., Pascanu, R., and Hadsell, R. Progressive neural networks. *arXiv preprint arXiv:1606.04671*, 2016.
- Schuhmann, C., Beaumont, R., Vencu, R., Gordon, C., Wightman, R., Cherti, M., Coombes, T., Katta, A., Mullis, C., Wortsman, M., Schramowski, P., Kundurthy, S., Crowson, K., Schmidt, L., Kaczmarczyk, R., and Jitsev, J. Laion-5b: An open large-scale dataset for training next generation image-text models. *ArXiv*, abs/2210.08402, 2022. URL <https://api.semanticscholar.org/CorpusID:252917726>.
- Sekharia, A., Acharya, J., Kamath, G., and Suresh, A. T. Remember what you want to forget: Algorithms for machine unlearning. *Advances in Neural Information Processing Systems*, 34:18075–18086, 2021.
- Sener, O. and Koltun, V. Multi-task learning as multi-objective optimization. *Advances in neural information processing systems*, 31, 2018.
- Siroš, I., Singelée, D., and Preneel, B. Github copilot: the perfect code completer? *arXiv preprint arXiv:2406.11326*, 2024.
- Sun, X., Panda, R., and Feris, R. S. Adashare: Learning what to share for efficient deep multi-task learning. In *Advances in Neural Information Processing Systems*, volume 33, pp. 8728–8740, 2020.
- Thiel, D. Identifying and eliminating csam in generative ml training data and models. Technical report, Stanford University, 2023. <https://purl.stanford.edu/kh752sm9123>.
- Thudi, A., Deza, G., Chandrasekaran, V., and Papernot, N. Unrolling sgd: Understanding factors influencing machine unlearning. In *2022 IEEE 7th European Symposium on Security and Privacy (EuroS&P)*, pp. 303–319. IEEE, 2022.
- Wang, J., Guo, S., Xie, X., and Qi, H. Federated unlearning via class-discriminative pruning. In *Proceedings of the ACM Web Conference 2022*, pp. 622–632, 2022.
- Wang, Z., Lipton, Z., and Tsvetkov, Y. Gradient vaccine: Investigating and improving multi-task optimization in massively multilingual models. In *International Conference on Learning Representations*, 2021.
- Wu, G., Hashemi, M., and Srinivasa, C. Puma: Performance unchanged model augmentation for training data removal.

In *Proceedings of the AAAI conference on artificial intelligence*, volume 36, pp. 8675–8682, 2022.

Wu, J. and Harandi, M. Scissorhands: Scrub data influence via connection sensitivity in networks. In *European Conference on Computer Vision*, pp. 367–384. Springer, 2025.

Yu, T., Kumar, S., Gupta, A., Levine, S., Hausman, K., and Finn, C. Gradient surgery for multi-task learning. *Advances in Neural Information Processing Systems*, 33: 5824–5836, 2020.

Zeng, G., Chen, Y., Cui, B., and Yu, S. Continual learning of context-dependent processing in neural networks. *Nature Machine Intelligence*, 1(8):364–372, 2019.

Zhang, Y. and Yang, Q. A survey on multi-task learning. *IEEE transactions on knowledge and data engineering*, 34(12):5586–5609, 2021.

Zhang, Y., Zhang, Y., Yao, Y., Jia, J., Liu, J., Liu, X., and Liu, S. Unlearncanvas: A stylized image dataset to benchmark machine unlearning for diffusion models. *arXiv preprint arXiv:2402.11846*, 2024.

A. Experimental Details

A.1. Image classification

We provide additional details about the image classification machine unlearning setup, including general information and the hyperparameter search performed for each method. This setup leverages the splits from the CIFAR10 and ImageNet datasets, focusing on either random unlearning samples or specific class samples. Results are reported across three random seeds or three different classes. All methods are trained for 30 epochs, with each setup utilizing its corresponding stopping criteria as explained in 5.2.

OrthoGrad. We performed grid search for the combination (α) and learning rate (η), and batch sizes for \mathcal{D}_u and \mathcal{D}_r . We apply LoRA modules to all linear layers within the self-attention and cross-attention layers. We set the rank to 8 and the scaling factor to 32. Specifically, for α , we searched over $\{0.9, 0.8\}$, and for η , we searched over $\{0.001, 0.01\}$. For the retain batch size, we considered $\{256, 128\}$, and for the unlearn batch size, we searched over $\{256, 128\}$. **For ViT architecture** The optimal parameters for random and class forgetting respectively $\alpha = (0.9, 0.8)$, $\eta = (0.001, 0.001)$, retain batch size = (128, 256), unlearn batch size = (128, 256). **For ResNet18 architecture** The optimal parameters for random and class forgetting respectively $\alpha = (0.9, 0.8)$, $\eta = (0.001, 0.001)$, retain batch size = (256, 256), unlearn batch size = (128, 256).

NegGrad. We performed grid search for learning rate (η), and batch size for \mathcal{D}_u . Specifically, for η , we searched over $\{1e - 3, 1e - 4, 1e - 5, 1e - 6\}$, and for unlearn batch size, we searched over $\{256, 128\}$. **For ViT architecture** The optimal parameters for random and class forgetting respectively $\eta = (1e - 4, 1e - 4)$, unlearn batch size = (256, 128). **For ResNet18 architecture** The optimal parameters for random and class forgetting respectively $\eta = (1e - 5, 1e - 5)$, unlearn batch size = (128, 256).

NegGrad+. We performed grid search for learning rate (η), and batch sizes for \mathcal{D}_u and \mathcal{D}_r . Specifically, for η , we searched over $\{1e - 3, 1e - 4, 1e - 5, 1e - 6\}$. For the retain batch size, we considered $\{256, 128\}$, and for unlearn batch size, we searched over $\{256, 128\}$. **For ViT architecture** The optimal parameters for random and class forgetting respectively $\eta = (1e - 3, 1e - 3)$, retain batch size = (128, 256), unlearn batch size = (128, 256). **For ResNet18 architecture** The optimal parameters for random and class forgetting respectively $\eta = (1e - 6, 1e - 5)$, retain batch size = (256, 256), unlearn batch size = (256, 256).

Fisher. We performed grid search for (α), and batch size for \mathcal{D}_r . Specifically, for α , we searched over $\{1e - 7, 1e - 8, 1e - 9\}$, and for retain batch size, we searched over $\{128, 256\}$. **For ViT architecture** The optimal parameters for random and class forgetting respectively $\eta = (1e - 9, 1e - 9)$, retain batch size = (128, 256). **For ResNet18 architecture** The optimal parameters for random and class forgetting respectively $\eta = (1e - 9, 1e - 9)$, retain batch size = (128, 256).

Influence. We performed grid search for (α), and batch sizes for \mathcal{D}_u and \mathcal{D}_r . Specifically, for α , we searched over $\{1, 0.1, 0.01, 1e - 3\}$. For the retain batch size, we considered $\{64, 128, 256\}$, and for unlearn batch size, we searched over $\{64, 128, 256\}$. **For ViT architecture** The optimal parameters for random and class forgetting respectively $\eta = (1, 1)$, retain batch size = (256, 128) and for unlearn batch size = (128, 128). **For ResNet18 architecture** The optimal parameters for random and class forgetting respectively $\eta = (0.001, 1)$, retain batch size = (64, 256) and for unlearn batch size = (256, 128).

SCRUB. We performed grid search for learning rate (η), and batch sizes for \mathcal{D}_u and \mathcal{D}_r . Specifically, for η , we searched over $\{5e - 2, 5e - 5 - 3, 5e - 4\}$. For the retain batch size, we considered $\{256, 512\}$, and for unlearn batch size, we searched over $\{256, 512\}$. **For ViT architecture** $\eta = 5e - 3$ retain batch size = 256, unlearn batch size = 512. **For ResNet18 architecture** $\eta = 5e - 4$ retain batch size = 256, unlearn batch size = 512.

DUCK. We performed grid search for learning rate (η), and batch sizes for \mathcal{D}_u and \mathcal{D}_r . Specifically, for η , we searched over $\{2e - 4, 5e - 4, 5e - 5\}$. For the retain batch size, we considered $\{128, 1024\}$, and for unlearn batch size, we searched over $\{128, 1024\}$. **For ViT architecture** $\lambda_{fgt} = (1.5, 0.5)$, $\lambda_{ret} = (1.5, 1.5)$, batch ratio = (5, 30), $\eta = (5e - 5, 2e - 4)$, retain and unlearn batch size = (128, 128), $\tau = (3, 3)$. **For ResNet18 architecture** $\lambda_{fgt} = (1.5, 0.5)$, $\lambda_{ret} = (1.5, 1.5)$, batch ratio = (5, 30), $\eta = (5e - 4, 2e - 4)$, retain and unlearn batch size = (1024, 1024), temperature = (3, 3).

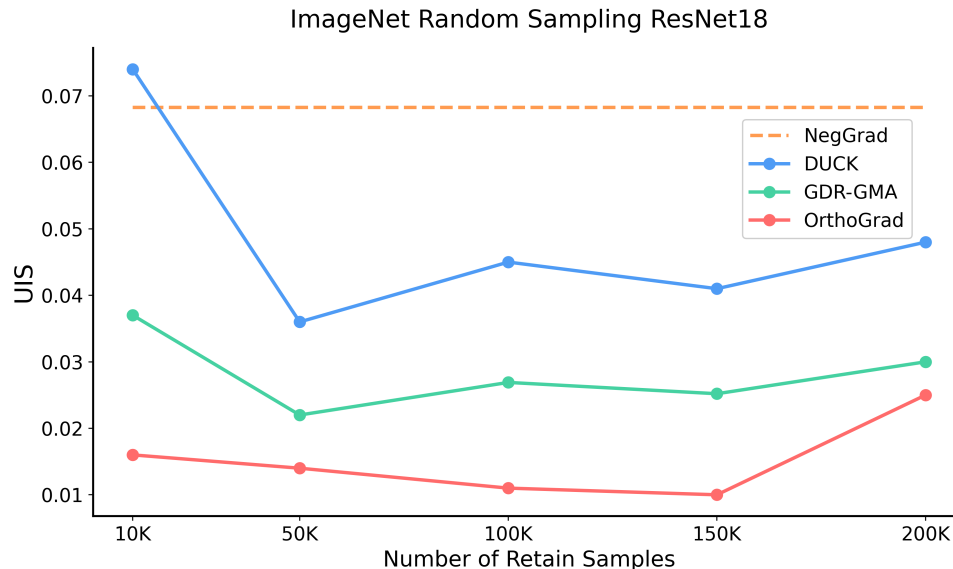


Figure 3. Performance comparison of different gradient-based methods on ImageNet with ResNet18 architecture. We report UIS values across varying numbers of retained samples.

GDR-GMA. We performed grid search for learning rate (η), and batch sizes for \mathcal{D}_u and \mathcal{D}_r . Specifically, for η , we searched over $\{1e-3, 1e-4, 1e-5\}$. For the retain batch size, we considered $\{128, 256\}$, and for unlearn batch size, we searched over $\{128, 256\}$. For all setups and architectures $\eta = 1e-4$ retain batch size = 256, unlearn batch size = 256.

A.2. Automatic Speech Recognition

Here, we present additional details about the ASR machine unlearning setup. This includes both general information about the setup and the hyperparameter search conducted for each method. In this setup, we utilized the train-100 split from the LibriSpeech dataset, targeting unlearning samples from a single speaker. The results are reported across 5 randomly sampled speakers. For all methods, we utilize a batch size of 48 for the retain and unlearn sets and 30 epochs with early stopping. In addition, we use the well-known Adam (Kingma, 2014) as the optimizer.

OrthoGrad. - We performed grid search for the combination (α) and learning rate (η) parameters. Specifically for α we searched over $\{0.05, 0.2, 0.35, 0.5\}$ and $\{1e-5, 5e-6, 1e-6\}$ for η . We apply LoRA modules to all linear layers within the self-attention and cross-attention layers. We set the rank to 8 and the scaling factor to 32.

Finetune. We performed a grid search for the learning rate parameter. Specifically, we explored learning rates in the range $\{1e-5, 5e-6, 1e-6\}$, and the optimal learning rate chosen is $\eta = 1e-5$.

NegGrad+. - We performed a grid search for the learning rate parameter. Specifically we searched over $\{1e-5, 5e-6, 2.5e-5, 1e-6, 5e-7, 1e-7\}$, and the optimal learning rate chosen is $5e-6$.

SCRUB. We performed a grid search for the learning rate and the number of epochs in which SCRUB performs unlearning steps. We searched over the range $[1e-4, 1e-7]$ with a step size of 0.5 in multiplication, as well as $\{10, 20, 30\}$ for the number of unlearning epochs. We observed that SCRUB either failed to achieve unlearning entirely or caused the model to collapse, resulting in poor generalization. We report the results with $1e-5$ learning and 20 unlearning epochs. We also used temperature rescaling of 4 in the knowledge distillation loss and $5e-4$ weight decay.

GDR-GMA. We performed a grid search for the learning rate and learning rate scheduling factor parameters. We searched over the range $[1e-4, 1e-7]$ with a step size of 0.5 in multiplication, and found the optimal learning rate to be $1e-4$. We explored learning rate scheduling factors in the set $\{10, 50, 100, 200\}$ and identified 100 as the optimal value.

A.3. Data preprocessing

We adopt the data preprocessing approach outlined by (Radford et al., 2023). The audio samples are resampled to 16 kHz, and log-magnitude Mel-spectrograms are generated. Specifically, we compute 80-channel Mel-spectrograms using 25-millisecond windows with a 10-millisecond stride.